

基于 2-氨基-3-羟基-吡啶 Schiff 碱的双核 Ni(II)和 Zn(II)配合物： 合成、超分子结构和光谱性质

常 健 张宏佳 贾浩然 孙银霞*

(兰州交通大学化学与生物工程学院,兰州 730070)

摘要: 合成了 2 个 2-氨基-3-羟基-吡啶 Schiff 碱双核 Ni(II)和 Zn(II)配合物, $[\text{Ni}(\text{L}^1)(\text{DMF})]_2$ (**1**) ($\text{H}_2\text{L}^1=4\text{-羟基-3-((3-羟基-吡啶-2-亚氨基))-苯并吡喃-2-酮}$)和 $[\text{Zn}(\text{L}^2)(\text{H}_2\text{O})]_2 \cdot 2\text{DMF}$ (**2**) ($\text{H}_2\text{L}^2=2\text{-((3,5-二溴-2-羟基)-氨基)-吡啶-3-醇}$), 并通过元素分析、红外光谱、紫外-可见吸收光谱、荧光光谱及 X 射线单晶衍射分析等手段进行了表征。X 射线单晶衍射分析结果表明: 配合物 **1** 和 **2** 均具有双核结构, 均由 2 个金属离子和 2 个配体单元以及 2 个配位的溶剂分子组成, 不同的是配合物 **2** 含有 2 个溶剂分子。配合物 **1** 和 **2** 都是单斜晶系、 $P2_1/c$ 空间群, 且中心金属 Ni(II)和 Zn(II)离子的空间构型均为五配位的扭曲的四方锥。此外, 配合物 **1** 和 **2** 通过分子间氢键、 $\text{C-H}\cdots\pi$ 及 $\pi\cdots\pi$ 作用形成 3D 超分子结构。此外, 讨论了 H_2L^1 , H_2L^2 及其相应的 Ni(II)和 Zn(II)配合物的荧光性质。配体 H_2L^1 和 H_2L^2 呈现蓝色发射, 最大发射波长 λ_{em} 分别为 457 和 473 nm, 而配合物 **1** 和 **2** 显示绿色发射, λ_{em} 分别为 543 和 538 nm。

关键词: 2-氨基-3-羟基-吡啶 Schiff 碱; 双核配合物; 超分子结构; 荧光性质

中图分类号: O614.81*3; O614.24*1

文献标识码: A

文章编号: 1001-4861(2018)11-2097-11

DOI: 10.11862/CJIC.2018.256

Binuclear Nickel(II) and Zinc(II) Complexes Based on 2-Amino-3-hydroxy-pyridine Schiff Base: Syntheses, Supramolecular Structures and Spectral Properties

CHANG Jian ZHANG Hong-Jia JIA Hao-Ran SUN Yin-Xia*

(School of Chemical and Biological Engineering, Lanzhou Jiaotong University, Lanzhou 730070, China)

Abstract: Two 2-amino-3-hydroxy-pyridine Schiff base binuclear Ni(II) and Zn(II) complexes, $[\text{Ni}(\text{L}^1)(\text{DMF})]_2$ (**1**) ($\text{H}_2\text{L}^1=4\text{-hydroxy-3-((3-hydroxy-pyridin-2-ylimino)-methyl)-chromen-2-one}$) and $[\text{Zn}(\text{L}^2)(\text{H}_2\text{O})]_2 \cdot 2\text{DMF}$ (**2**) ($\text{H}_2\text{L}^2=2\text{-((3,5-dibromo-2-hydroxy-benzylidene)-amino)-pyridin-3-ol}$) have been synthesized and characterized by elemental analyses, IR, UV-Vis, emission spectra and X-ray crystallography. X-ray crystallography analyses showed that complexes **1** and **2** all possess the binuclear structures, consisting of two metal ions, two ligand units and two coordinated solvent molecules, in which the difference is that complex **2** contains two solvent molecules. Complexes **1** and **2** crystallize in the monoclinic space group $P2_1/c$ and the center Ni(II) and Zn(II) are all five-coordinated slightly distorted square pyramid geometry by four O atoms and one imine N atoms. Complex **1** (or **2**) links some other molecules into an infinite 3D network supramolecular structure via intermolecular hydrogen bond, $\text{C-H}\cdots\pi$ or $\pi\cdots\pi$ stacking interactions. And the fluorescent properties of H_2L^1 , H_2L^2 and their corresponding Ni(II) and Zn(II) complexes have been discussed. The ligands H_2L^1 and H_2L^2 exhibit blue emission with the maximum emission wavelength $\lambda_{\text{em}}=457$ and 473 nm, and complexes **1** and **2** show green emission with $\lambda_{\text{em}}=543$ and 538 nm. CCDC: 1855900, **1**; 1855901, **2**.

Keywords: 2-amino-3-hydroxy-pyridine Schiff base; binuclear complex; supramolecular structure; fluorescence property

收稿日期: 2018-07-14。收修改稿日期: 2018-09-11。

兰州交通大学优秀科研平台(No.201706)、甘肃省重点研发计划项目(No.18YF1GA054)资助。

*通信联系人。E-mail: sun_yinxia@163.com; 会员登记号: 02M100427534。

0 Introduction

Schiff base compounds and their transition metal complexes are playing an important part in the development of coordination chemistry^[1-5] because of their potential application in catalysis^[6], bioscience^[7-11], magnetic materials^[12-17], luminescent^[18-24], electrochemical systems^[25-26] and constructing supramolecular structures building^[27-33]. There have been reports of the use of Schiff base ligands synthesized from salicylaldehyde and various amines to form complexes with transition metals such as complexes of nickel(II)^[35] and copper(II)^[36-38]. In recent years, there has been enhanced interest in the synthesis and characterization of such complexes due to their interesting properties and other applications^[39-46]. Herein, in order to further study the supramolecular of the transition metal complexes with the Schiff base ligand, we synthesized and analyzed two complexes, $[\text{Ni}(\text{L}^1)(\text{DMF})_2]$ (**1**) (H_2L^1 =4-hydroxy-3-((3-hydroxy-pyridin-2-ylimino)-methyl)-chromen-2-one) and $[\text{Zn}(\text{L}^2)(\text{H}_2\text{O})_2 \cdot 2\text{DMF}]$ (**2**) (H_2L^2 =2-((3,5-dibromo-2-hydroxy-benzylidene)-amino)-pyridin-3-ol), which was named complexes **1** and **2**. Complexes **1** and **2** are all binuclear structures and links some other molecules into an infinite 3D network supramolecular structure via intermolecular hydrogen bond, $\text{C}-\text{H} \cdots \pi$ or $\pi \cdots \pi$ stacking interactions. The ligands H_2L^1 and H_2L^2 exhibit blue emission and complexes **1** and **2** all show green emission with λ_{em} =543 and 538 nm.

1 Experimental

1.1 Materials

4-hydroxyl coumarin, POCl_3 , 2-amino-3-hydroxypyridine ($\geq 98\%$) from Alfa Aesar was used without further purification. The other reagents and solvents were of analytical grade from Tianjin Chemical Reagent Factory.

1.2 Methods

C, H and N analyses were carried out with a GmbH VariuoEL V3.00 automatic elemental analyzer. IR spectra were recorded on a Vertex70 FT-IR spectrophotometer, with samples prepared as KBr ($400 \sim 4000 \text{ cm}^{-1}$) pellets. UV-Vis absorption spectra

were recorded on a Shimadzu UV-3900 spectrometer. Luminescence spectra in solution were recorded on a Hitachi F-7000 spectrometer. Melting points were measured by the use of a microscopic melting point apparatus made by Beijing Taike Instrument Limited Company and were uncorrected.

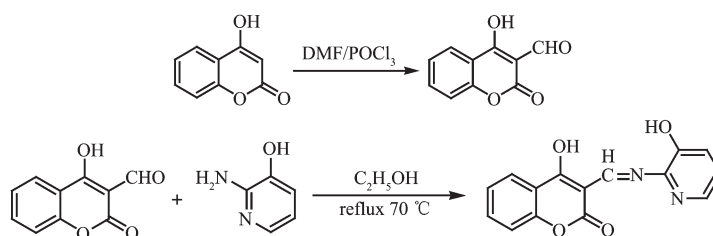
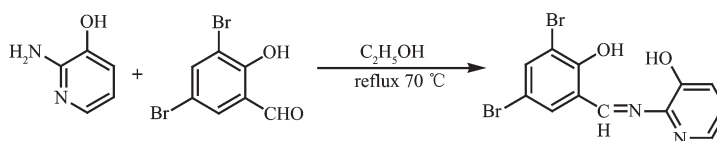
1.3 Syntheses of ligands H_2L^1 and H_2L^2

HL^1 and HL^2 were synthesized according to the following synthetic routes shown in Scheme 1 and 2.

H_2L^1 : 3-Formyl-4-hydroxyl-coumarin was synthesized according to the analogous method^[47]. POCl_3 (10 mL, 2.00 mmol) was dropped in the anhydrous DMF solution (10 mL) of 4-hydroxyl coumarin (3.8 g, 20.00 mmol) with the reaction temperature sustained lower than 5°C . The reaction mixture was kept at room temperature for 2 h, then it was heated in the steam bath for 1 h at 70°C . After the mixed solution come to room temperature, it was mixed with ice water and neutralized with sodium carbonate, and the resulting yellow solid was collected and recrystallized using ethyl alcohol. Yield: 78.6%; m.p. $115 \sim 116^\circ\text{C}$. Anal. Calcd. for $\text{C}_{10}\text{H}_6\text{O}_4$ (%): C, 63.16; H, 3.18. Found(%): C, 63.68; H, 3.21.

A solution of 3-formyl-4-hydroxyl coumarin (190.03 mg, 1.00 mmol) in ethanol (2 mL) was added to a solution of 2-amino-3-hydroxy pyridine (110.05 mg, 1.00 mmol) in ethanol (2 mL) and the mixture was subjected to heating at 70°C for 12 h. After the mixed solution come to room temperature, the resulting white solid was collected. After cooling to room temperature the light yellow precipitate was filtered and washed successively with ethanol/petroleum ether (1:4, V/V). The product was dried under reduced pressure to obtain 222.00 mg H_2L^1 . Yield: 74.5%. m.p. $214 \sim 215^\circ\text{C}$. Anal. Calcd. for $\text{C}_{15}\text{H}_{10}\text{N}_2\text{O}_4$ (%): C, 63.83; H, 3.57; N, 9.93. Found(%): C, 63.52; H, 4.22; N, 9.80.

H_2L^2 : The ligand H_2L^2 was synthesized by a method similar to that of H_2L^1 except substituting 3-aldehyde-4-hydroxy coumarin with 3,5-dibrominesalicylaldehyde. Yield: 351.33 mg, 76.8%. m.p. $204 \sim 205^\circ\text{C}$. Anal. Calcd. for $\text{C}_{12}\text{H}_8\text{Br}_2\text{N}_2\text{O}_2$ (%): C, 38.74; H, 2.17; N, 7.53. Found(%): C, 38.81; H, 2.16; N, 7.49.

Scheme 1 Synthetic route of H_2L^1 Scheme 2 Synthetic route of H_2L^2

1.2.2 Syntheses of complexes **1** and **2**

Complex 1: A solution of Ni(II) acetate monohydrate (0.7 mg, 0.003 mmol) in ethanol (2 mL) was added dropwise to a solution of H_2L^1 (0.95 mg, 0.005 mmol) in acetone (4 mL). The color of the mixture turned to brown immediately, and then 2 drops of DMF were added in it, stirred for 1 h at room temperature. The mixture was filtered, and the filtrate was allowed to stand at room temperature for about a week. The solvent was partially evaporated, and single crystals suitable for X-ray crystallographic analysis were obtained. Yield: 25.6%. Anal. Calcd. for $C_{18}H_{15}N_3NiO_5$ (%): C, 52.47; H, 3.67; N, 10.20. Found(%): C 53.47, H, 3.67; N, 10.87.

Complex 2: The complex **2** was synthesized with the similar method for complex **1**. Yield: 28.6%. Anal. Calcd. for $C_{15}H_8Br_2N_2O_4Zn$ (%): C, 34.22; H, 2.87; N, 7.98. Found(%): C, 34.78; H, 2.87; N, 8.38.

1.3 Crystal structure determinations of complexes **1** and **2**

The single crystals of the complexes with approximate dimensions of 0.40 mm × 0.11 mm × 0.08 mm (**1**) and 0.30 mm × 0.27 mm × 0.15 mm (**2**) were placed on a Bruker Smart 1000 CCD area detector. The reflections were collected using graphite-monochromatized Mo $K\alpha$ radiation ($\lambda = 0.071\ 073$ nm). The Lp corrections were applied to the SAINT program^[48] and semi-empirical correction were applied to the SADABS program^[49]. The crystal structures were solved by the direct methods (SHELXS-2014)^[50]. The hydrogen atoms of water molecules in the complex **2** were located from difference Fourier maps, and the other hydrogen atoms were generated geometrically. Details of the crystal parameters, data collection and refinements for complexes **1** and **2** are summarized in Table 1.

CCDC: 1855900, **1**; 1855901, **2**.

Table 1 Crystal data and structure refinement for complexes **1** and **2**

Empirical formula	$C_{18}H_{15}N_3NiO_5$	$C_{12}H_8Br_2N_2O_4Zn \cdot C_3H_7NO$
Formula weight	412.04	526.49
Temperature / K	297.16(10)	293(2)
Crystal system	Monoclinic	Monoclinic
Space group	$P2_1/c$	$P2_1/c$
a / nm	0.991 21(4)	1.159 66(6)
b / nm	1.411 92(6)	1.394 83(4)
c / nm	1.240 16(5)	1.135 06(6)
β / (°)	102.395(5)	105.547(5)
Volume / nm ³	1.695(13)	1.768(14)
Z	4	4
D_c / (Mg · m ⁻³)	1.615	1.977

Continued Table 1

μ / mm^{-1}	1.18	5.93
$F(000)$	848	1 032
θ range / ($^{\circ}$)	3.566 0~28.422 0	3.679 0~23.951 0
Limiting indices	$-16 \leq h \leq 17, -12 \leq k \leq 13, -15 \leq l \leq 14$	$-14 \leq h \leq 7, -17 \leq k \leq 16, -13 \leq l \leq 14$
Reflection collected, unique	6 323, 2 737 ($R_{\text{int}}=0.026$)	7 039, 2 306 ($R_{\text{int}}=0.047$)
Completeness to $\theta=26.32^{\circ}$ / %	99.67	99.74
Data, restraint, parameter	3 335, 0, 246	3 478, 0, 229
GOF on F^2	1.047	0.912
$R_1, wR_2 [I > 2\sigma(I)]$	0.036 1, 0.081 5	0.053 3, 0.133 0
Largest diff. peak and hole / ($\text{e} \cdot \text{nm}^{-3}$)	520 and -322	836 and -766

2 Results and discussion

2.1 Crystal structures of complexes **1** and **2**

The single crystal structures and the coordination pattern diagram of complexes **1** and **2** are shown in Fig.1 and 2. The selected bond lengths and angles of complexes **1** and **2** are listed in Table 2. X-ray crystallographic analysis reveals that both complexes **1** and **2** crystallize in the monoclinic system with space group $P2_1/c$. Complexes **1** and **2** can be described as binuclear $M(\text{II})$ complexes ($M=\text{Ni}$ or Zn), consist of two $M(\text{II})$ ions, two (L^{2-}) units and two coordinated solvent molecules (DMF for **1** and H_2O for **2**), in which the

difference is that complex **2** contains two free DMF molecules.

As presented in Fig.1 and Fig.2, the $M(\text{II})$ ion (Ni for **1** and Zn for **2**) was coordinated by one oxime nitrogen (N1) atoms and two deprotonated hydroxyl oxygen (O3 , O4 in **1** and O1 , O2 in **2**) atoms of (L^{2-}) units ($\text{L}=\text{L}^1$ or L^2), as well as one oxygen (O5 in **1** and O4 in **2**) atom of the coordinated solvent molecule (DMF for **1** and H_2O for **2**), which constitute the $[\text{M}(\text{L})(\text{solvent})]$ moiety. And then the O4 and O4A in **1** (and O2 and O2A in **2**) atoms bridge the two $[\text{M}(\text{L})(\text{solvent})]$ moieties to form the binuclear structure $[\text{Ni}(\text{L}^1)(\text{DMF})]_2$ (**1**) and $[\text{Zn}(\text{L}^2)(\text{H}_2\text{O})]_2$ (**2**). Thus, the

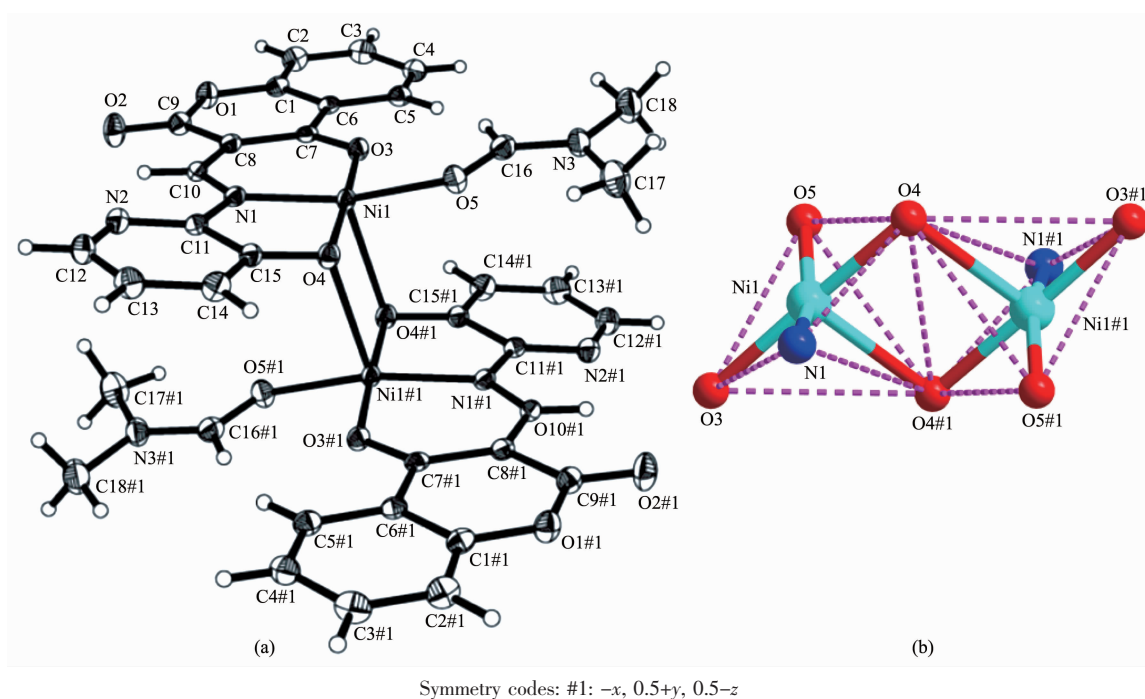


Fig.1 (a) Molecular structure of complex **1** showing 30% probability displacement ellipsoids;
(b) Coordination geometry diagram for $\text{Ni}(\text{II})$ ions of complex **1**

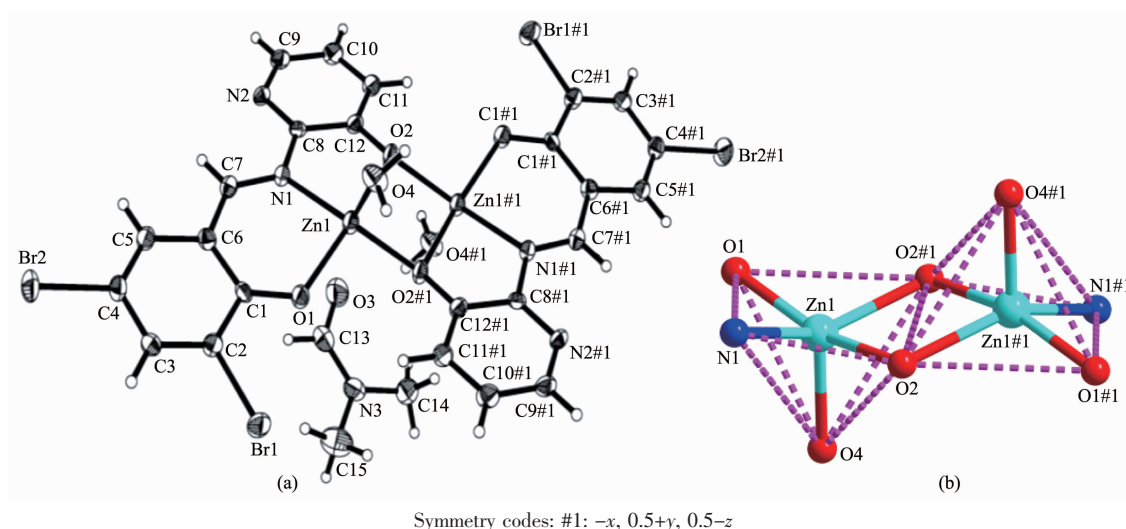


Fig.2 Molecular structure of complex **2** showing 30% probability displacement ellipsoids;
(b) Coordination geometry diagram for Zn(II) ions of complex **2**

Table 2 Selected bond lengths (nm) and bond angles ($^{\circ}$) for complexes **1** and **2**

Complex 1					
Ni1-O3	0.194 0(2)	Ni1-O5	0.197 8(2)	Ni1-O4#1	0.235 8(2)
Ni1-O4	0.194 4(2)	Ni1-N1	0.192 9(2)		
O3-Ni1-O5	94.25(8)	O3-Ni1-O4	177.77(7)	O3-Ni1-O4#1	92.27(7)
O5-Ni1-O4#1	89.16(7)	O4-Ni1-O5	87.94(7)	O4-Ni1-O4#1	87.37(7)
N1-Ni1-O3	93.03(8)	N1-Ni1-O5	161.42(8)	N1-Ni1-O4#1	107.62(7)
N1-Ni1-O4	84.99(8)	Ni1-O4-Ni1#1	92.63(7)	C7-O3-Ni1	126.33(2)
Complex 2					
Zn1-O1	0.196 5(5)	Zn1-O2#1	0.200 0(4)	Zn1-O2	0.209 8(4)
Zn1-O4	0.201 7(5)	Zn1-N1	0.206 1(5)	O2-Zn1#1	0.200 0(4)
O1-Zn1-O2#1	100.8(2)	O1-Zn1-O2	161.30(2)	O1-Zn1-O4	101.39(2)
O1-Zn1-N1	90.62(2)	O2#1-Zn1-O2	78.33(2)	O2#1-Zn1-O4	103.22(2)
O2#1-Zn1-N1	140.7(2)	O4-Zn1-O2	96.95(2)	O4-Zn1-N1	111.22(2)

Symmetry codes: #1: $-x, 0.5+y, 0.5-z$ for complexes **1** and **2**.

central M(II) ions are penta-coordinated and their coordination sphere is best described as a distorted tetragonal pyramid. In order to get the geometry adopted by M(II) ions, the τ value was estimated to be $\tau=0.222\ 8$ for **1** and $\tau=0.133\ 3$ for **2**^[51-52]. The difference between complexes **1** and **2** is that the two [M(L)] moieties in complex **2** are almost planar with the distance of 0.007 7 nm but those in **1** are paralleled with the distance of 0.251 0 nm. As well as in complex **1** the coordinated DMF molecule is almost planar with [Ni(L¹)] moiety but the coordinated H₂O

molecule in complex **2** is almost perpendicular to the [Zn(L²)] moiety.

2.2 Intermolecular interactions of complexes **1** and **2**

The intra- and intermolecular interactions data of complexes **1** and **2** are shown in Table 3 and 4. The crystal structure of complex **1** is stabilized by a pair of intramolecular non-classic hydrogen bonds C16-H16 \cdots O3 (Fig.3, Table 3). Meanwhile, two pairs of intermolecular C18-H18B \cdots O2 and C12-H12 \cdots O4 hydrogen bonds link neighboring molecules into 2D

Table 3 Hydrogen-bonding interactions for complexes **1** and **2**

D-H...A	<i>d</i> (D-H) / nm	<i>d</i> (H...A) / nm	<i>d</i> (D...A) / nm	∠ D-H...A / (°)
Complex 1				
C16-H16...O3	0.093	0.241	0.297 4(3)	119
C12-H12...O4#1	0.093	0.246	0.337 6(3)	169
C18-H18B...O2#2	0.096	0.252	0.346 2(4)	166
Complex 2				
C5-H5...O3#1	0.093	0.247	0.335 6(9)	159
O4-H4A...O3#2	0.086	0.183	0.265 0(9)	158
O4-H4B...N2#3	0.086	0.202	0.275 9(7)	143
C15-H15C...Cg5#4	0.096	0.271	0.361 5(11)	161
C14-H14C...Cg6#5	0.096	0.300	0.381 3(10)	144

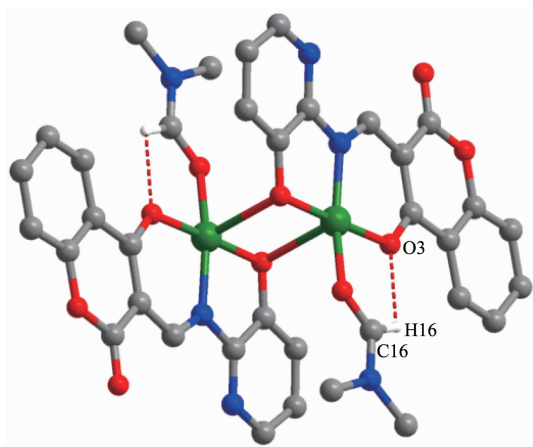
Cg5 and Cg6 are the centroids of benzene ring C1#4-C6#4 and the chelate ring C8#5-C12#5-O2#5-Zn1#5-N1#5 of complex **2**, respectively; Symmetry codes: #1: $x, 1/2-y, -1/2+z$; #2: $x, y, 1+z$ for **1**; #1: $x, 1/2-y, -1/2+z$; #2: $-x, -y, 2-z$; #3: $-x, -1/2+y, 3/2-z$; #4: $1-x, -y, 2-z$; #5: $-x, -y, 2-z$ for **2**.

Table 4 $\pi \cdots \pi$ stacking interactions for complex **1**

Ring (<i>i</i>)	Ring (<i>j</i>)	<i>d</i> (Cg...Cg) / nm	<i>d</i> (Cg(<i>i</i>)-perp) / nm	<i>d</i> (Cg(<i>j</i>)-perp) / nm
Cg1	Cg4#3	0.360 38(15)	0.332 92(9)	0.327 87(11)
Cg2	Cg4#3	0.349 87(14)	0.330 91(8)	0.331 93(11)
Cg2	Cg3#3	0.367 44(13)	0.328 74(9)	0.330 08(10)

Cg1, Cg2, Cg3#3 and Cg4#3 are the centroids of ring C11-N1-Ni1-O4-C15, C7-O3-Ni1-N1-C10, C1#3-O1#3-C9#3 and C1#3-C6#3, respectively; Symmetry codes: #3: $1-x, -y, 1-z$.

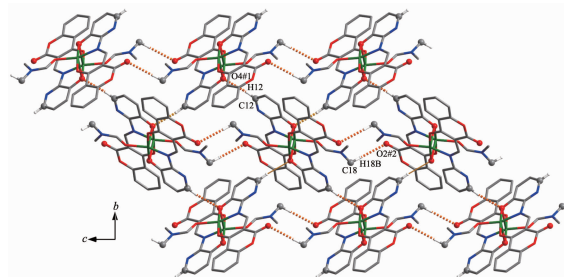
supramolecular network structure parallel to the *bc* planes (Fig.4). Synchronously, complex **1** molecules are further linked by three pairs of intermolecular $\pi \cdots \pi$ stacking interactions (Cg1...Cg4, Cg2...Cg4 and Cg2...Cg3) between the benzene ring of adjacent complex **1** molecules to form the other 1D infinite chain along *a* axis (Fig.5, Table 4). Thus, complex **1**



Hydrogen atoms, except those forming hydrogen bonds, are omitted for clarity

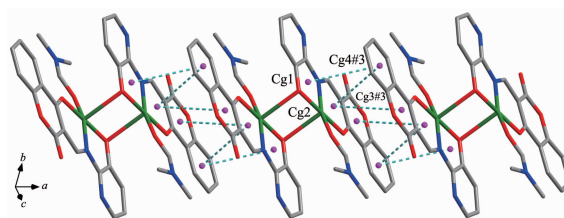
Fig.3 Intramolecular hydrogen bonding of complex **1**

molecules self-assemble via the intermolecular non-classic hydrogen-bonding and $\pi \cdots \pi$ stacking interactions



Symmetry codes: #1: $x, 1/2-y, -1/2+z$; #2: $x, y, 1+z$

Fig.4 Part of 2D supramolecular structure of complex **1** linked by intermolecular hydrogen bonds parallel to the *bc* planes



Symmetry codes: #3: $1-x, -y, 1-z$

Fig.5 Part of 1D supramolecular structure linked by $\pi \cdots \pi$ stacking interactions along the *a* axis of complex **1**

tions to form the 3D supramolecular networks structure (Fig.6). Consequently, the intermolecular non-classical hydrogen-bonding and $\pi \cdots \pi$ stacking interactions plays a very important role in the construction of supramolecular networks structure^[53-59].

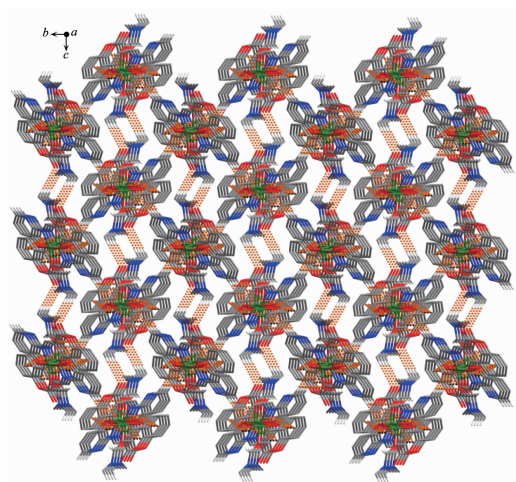
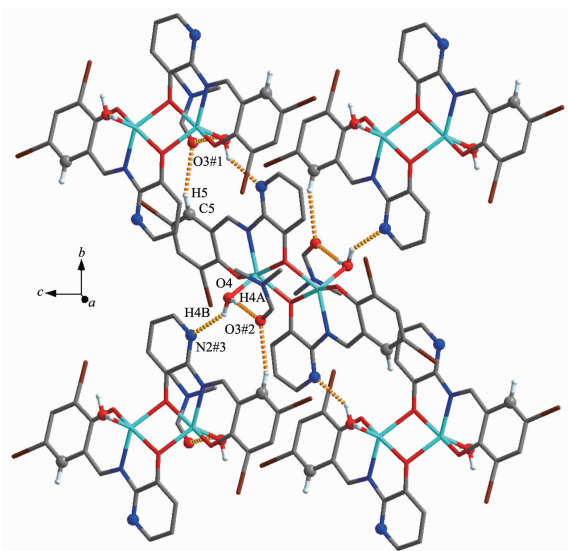


Fig.6 Part of a self-assembling 3D supramolecular structure of complex **1**

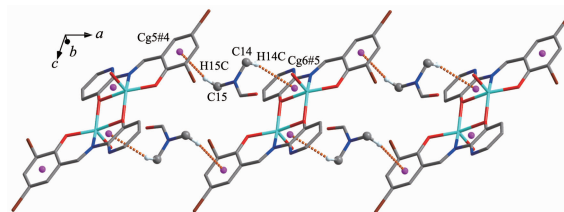
Complex **2** contains crystallizing DMF molecules and the oxygen atoms (O3) of the crystallizing DMF molecules have hydrogen-bond interactions with the coordinated water molecules and benzene rings of the L^{2-} unit of one neighboring complex molecule, respec-



Symmetry codes: #1: $x, 1/2-y, -1/2+z$; #2: $-x, -y, 2-z$; #3: $-x, -1/2+y, 3/2-z$

Fig.7 Part of 2D supramolecular structure linked by intermolecular hydrogen bonds parallel to the bc planes of complex **2**

tively. Meanwhile, the coordinated water molecules are bonded to the neighboring complex molecule. Thus, the complex molecules and the crystallizing DMF molecules are linked by intermolecular hydrogen bonds to form a 2D-layer supramolecular structure parallel to the bc planes (Fig.7, Table 3). Furthermore, this linkage is further stabilized by two pairs of intermolecular hydrogen bonds interactions ($C15-H15C \cdots Cg5$ and $C14-H14C \cdots Cg6$), which interlink the neighboring molecules into the other 1D infinite chain along the a axis (Fig.8, Table 3). Thus, the crystal packing of complex **2** shows that a 3D supramolecular networks are formed through intermolecular $O-H \cdots O$, $O-H \cdots N$, $C-H \cdots O$ and $C-H \cdots \pi$ hydrogen bonding interactions^[60-66] (Fig.9).



Symmetry codes: #4: $1-x, -y, 2-z$; #5: $-x, -y, 2-z$

Fig.8 Part of 1D supramolecular structure linked by $C-H \cdots \pi$ stacking interactions along the a axis of complex **2**

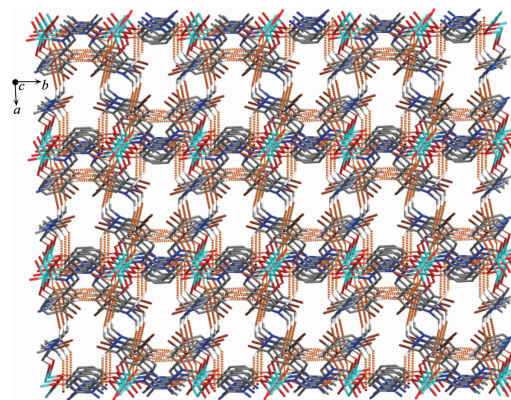


Fig.9 Part of self-assembling 3D supramolecular structure of complex **2**

2.3 IR spectra analyses

The FT-IR spectra of H_2L^1 , H_2L^2 and their corresponding complexes **1** and **2** exhibit various bands in the $400 \sim 4\,000\text{ cm}^{-1}$ region. The most important FT-IR bands for H_2L^1 , H_2L^2 and its Ni(II) and Zn(II) complexes are listed in Table 5.

Table 5 Main bands in IR spectra of H_2L^1 , H_2L^2 and their Ni(II) and Zn(II) complexes

Compound	$\nu(\text{O-H})$	$\nu(\text{C=N})$	$\nu(\text{Ar-O})$	$\nu(\text{M-N})$	$\nu(\text{M-O})$
H_2L^1	3 447	1 619	1 200	—	—
1	3 442	1 605	1 193	478	438
H_2L^2	3 460	1 607	1 203	—	—
2	3 437	1 600	1 196	576	506

The characteristic C=N stretching band of the free ligand H_2L^1 and H_2L^2 appeared at 1 619 and 1 607 cm^{-1} , respectively, while those of complexes **1** and **2** were observed in the 1 605 and 1 600 cm^{-1} , respectively^[67-75]. The C=N stretching frequencies were all shifted to lower frequencies by *ca.* 14 and 7 cm^{-1} upon complexation respectively, indicating a decrease in the C=N bond order due to the coordinated bond of the metal atom with the imino nitrogen lone pair^[76-78]. The Ar-O stretching band of the ligands H_2L^1 and H_2L^2 occurred at 1 200 and 1 203 cm^{-1} , respectively, and those at 1 193 and 1 196 cm^{-1} for complexes **1** and **2**. The lower frequency of the Ar-O absorption shift indicates that M-O bond is formed between the metal ions and the oxygen atoms of the phenolic groups^[59]. In addition, the broad O-H group stretching band at 3 447 and 3 460 cm^{-1} in the free ligands H_2L^1 and H_2L^2 disappeared in complexes **1** and **2**, indicating the oxygen atoms in the phenolic hydroxyl groups have been completely deprotonated and coordinated to the metal ions. Whereas, the stretching band at 3 437 cm^{-1} in the complex **2** is attributed to the stretching vibrations of the O-H group of the coordinated water. The FT-IR spectrum of complex **1** showed $\nu(\text{M-N})$ and $\nu(\text{M-O})$ vibration absorption frequencies at 478 and 438 cm^{-1} (or 576 and 506 cm^{-1} for complex **2**), respectively. These assignments are consistent with the literature frequency values.

2.4 UV-Vis spectra analyses

The absorption spectra of ligands H_2L^1 , H_2L^2 and their corresponding Ni(II) and Zn(II) complexes **1** and **2** were determined in diluted DMF solution as shown in Fig.10 and 11. The electronic absorption spectrum of free ligand H_2L^1 exhibited two absorption peaks at approximately 271 and 390 nm (Fig.10). The former absorption peaks at 271 nm can be assigned to the π -

π^* transition of the benzene rings and the latter at 390 nm can be attributed to the intraligand π - π^* transition of the C=N group^[79]. Upon coordination of the ligand, the relatively intense absorption at 390 nm disappeared from UV-Vis spectra of complex **1**, indicating that the amino nitrogen is involved in coordination with Ni(II) ion^[80]. The intraligand π - π^* transition of the benzene ring is bathochromically shifted to 310 nm in complex **1**, indicating the coordination of Ni(II) ion with deprotonated L^- unit. The new peak at 437 nm of complex **1** is assigned to $\text{L} \rightarrow \text{M}$ charge-transfer transition.

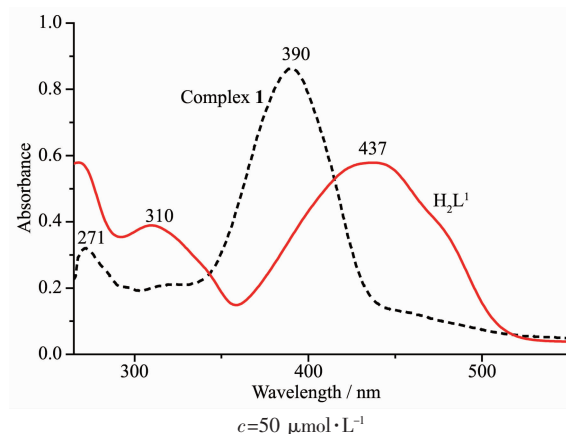


Fig.10 UV-Vis absorption spectra of H_2L^1 and complex **1** in diluted DMF solution at room temperature

The absorption of complex **2** was obviously different from that of H_2L^2 owing to complexation (Fig. 11). For the free ligand there were two intense peaks centered at around 275 and 399 nm, assigned to π - π^* transitions of the benzene rings of the benzaldehyde and C=N groups, respectively. Compared with the absorption peak of the free ligand, the absorption at 275 nm was slightly shifted hypsochromically to 272 nm of complex **2**, indicating the coordination of Zn(II) ion with deprotonated L^- unit. Meanwhile, the absorption peak at 399 nm disappeared from the UV-

Vis spectrum of complex **2**, which indicates that the amino nitrogen atom is involved in coordination to the metal atom. In addition, a new absorption peak was observed at 460 nm in complex **2**, which is assigned to the L \rightarrow M charge-transfer transition. This is characteristic of a transition metal complex with Schiff base ligand^[80].

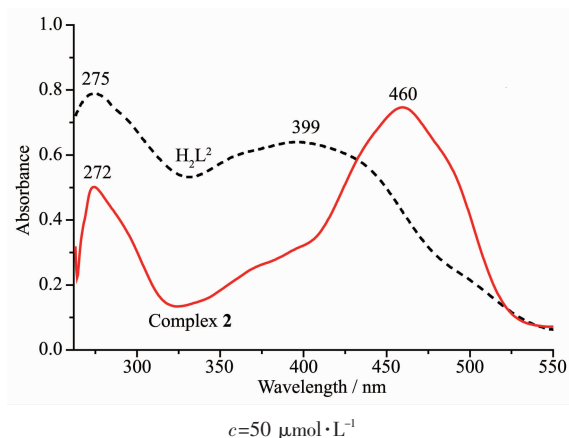


Fig.11 UV-Vis absorption spectra of H_2L^2 and complex **2** in diluted DMF solution at room temperature

2.5 Emission spectra of complexes **1** and **2**

The emission spectra of ligands H_2L^1 and H_2L^2 , complexes **1** and **2** were determined in diluted DMF solution at room temperature as shown in Fig.12 and 13. The ligands H_2L^1 and H_2L^2 exhibited the relatively weak emission at 457 and 473 nm upon excitation at 321 and 351 nm, respectively. The blue emission should be assigned to intraligand π - π^* transition^[81-82]. Compared with the free ligands H_2L^1 and H_2L^2 , an intense green emission at 543 and 538 nm for

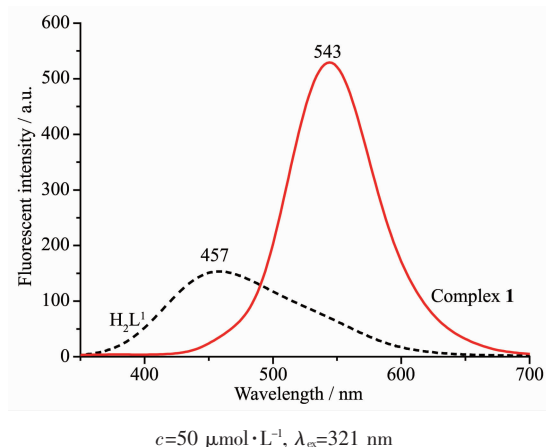


Fig.12 Emission spectra of H_2L^1 and complex **1** in diluted DMF at room temperature

complexes **1** and **2** were observed upon excitation at 321 and 351 nm, respectively, which indicates that the addition of metal ions Ni(II) and Zn(II) induces the change of the fluorescence characteristics of the ligand, which may be due to the destruction of the intramolecular hydrogen bonding of the ligand and resulting in the enhancement of the planarity of the conjugated system^[83-85]. The Stokes shift between the maximum wavelength of the fluorescence emission and the fluorescence excitation for H_2L^1 , complex **1**, H_2L^2 and complex **2** is 136, 222, 122 and 182 nm, respectively, which indicates that the introduction of coumarin group is beneficial to the luminescence of ligand and its metal complex. And the red shifts in emission wavelength of complexes **1** and **2** compared with H_2L^1 and H_2L^2 might be related to the coordination of the metal ions to the ligands and increases of the rigidity of ligands, which can diminish the loss of energy via vibrational motions and increase the emission efficiency.

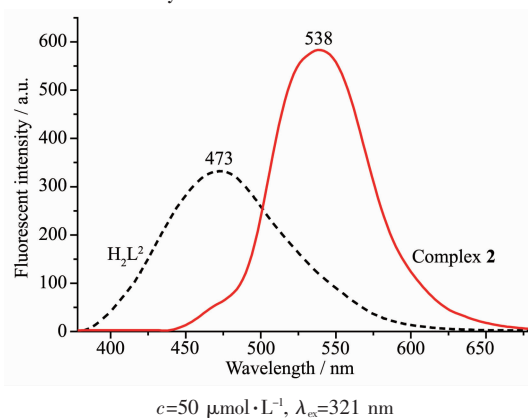


Fig.13 Emission spectra of H_2L^2 and complex **2** in diluted DMF at room temperature

3 Conclusions

The syntheses, structural characterizations, and fluorescence properties of the Schiff base ligands H_2L^1 , H_2L^2 and their corresponding binuclear Ni(II) and Zn(II) complexes **1** and **2** were discussed. Crystal structure analyses of complexes **1** and **2** showed that the Ni(II) and Zn(II) atoms all have penta-coordinate environments and adopt distorted square pyramidal geometries. Complexes **1** and **2** are self-assembled into the 3D supramolecular networks through intermolecular

hydrogen bonding, C-H $\cdots\pi$ and $\pi\cdots\pi$ stacking interactions. Furthermore, the optical properties of complexes **1** and **2** indicated that the coordination of metal ions Ni(II) and Zn(II) leads to the fluorescence enhancement of H₂L¹ and H₂L². Moreover, the Stokes shifts of H₂L¹ and complex **1** is larger than those of H₂L² and complex **2**, which indicates that the introduction of coumarin group is beneficial to the luminescence of ligand and its metal complex.

Acknowledgements: This work was supported by Gansu science and technology plan program (Grant No.18YF1GA054), and the Program for Excellent Team of Scientific Research in Lanzhou Jiaotong University (Grant No.201706), which is gratefully acknowledged.

References:

- [1] Liu Y A, Wang C Y, Zhang M, et al. *Polyhedron*, **2017**,**127**: 278-286
- [2] Dong W K, Ma J C, Dong Y J, et al. *Polyhedron*, **2016**,**115**: 228-235
- [3] SUN Yin-Xia(孙银霞), DONG Wen-Kui(董文魁), WANG Li(王莉), et al. *Chinese J. Inorg. Chem.*(无机化学学报), **2009**, **25**:1478-1482
- [4] Sun Y X, Zhang S T, Ren Z L, et al. *Synth. React. Inorg. Met.-Org. Nano-Met. Chem.*, **2013**,**43**:995-1000
- [5] YANG Yu-Hua(杨玉华), HAO Jing(郝静), DONG Yin-Juan(董银娟), et al. *Chinese J. Inorg. Chem.*(无机化学学报), **2017**,**33**:1280-1292
- [6] Wu H L, Pan G L, Bai Y C, et al. *J. Chem. Res.*, **2014**,**38**: 211-217
- [7] Yang H Q, Zhang L, Zhong L, et al. *Angew. Chem. Int. Ed.*, **2007**,**46**:6861-6865
- [8] Li X Y, Kang Q P, Liu L Z, et al. *Crystals*, **2018**,**8**:43
- [9] Wu H L, Pan G L, Bai Y C, et al. *Res. Chem. Intermed.*, **2015**,**41**:3375-3388
- [10] Chen C Y, Zhang J W, Zhang Y H, et al. *J. Coord. Chem.*, **2015**,**68**:1054-1071
- [11] Wu H L, Bai Y H, Zhang Y H, et al. *Z. Anorg. Allg. Chem.*, **2014**,**640**:2062-2071
- [12] Hao J, Li L L, Zhang J T, et al. *Polyhedron*, **2017**,**134**:1-10
- [13] Wu H L, Wang C P, Wang F, et al. *J. Chin. Chem. Soc.*, **2015**,**62**:1028-1034
- [14] Song X Q, Liu P P, Xiao Z R, et al. *Inorg. Chim. Acta*, **2015**, **438**:232-244
- [15] Dong W K, Li X L, Wang L, et al. *Sens. Actuators B: Chem.*, **2016**,**229**:370-378
- [16] Liu P P, Sheng L, Song X Q, et al. *Inorg. Chim. Acta*, **2015**, **434**:252-257
- [17] Dong W K, Ma J C, Zhu L C, et al. *New J. Chem.*, **2016**,**40**: 6998-7010
- [18] Zhang H, Dong W K, Zhang Y, et al. *Polyhedron*, **2017**,**133**: 279-293
- [19] Dong X Y, Akogun S F, Zhou W M, et al. *J. Chin. Chem. Soc.*, **2017**,**64**:412-419
- [20] Tao C H, Ma J C, Zhu L C, et al. *Polyhedron*, **2017**,**128**:38-45
- [21] Dong Y J, Dong X Y, Dong W K, et al. *Polyhedron*, **2017**, **123**:305-315
- [22] Li G, Hao J, Liu L Z, et al. *Crystals*, **2017**,**7**:217
- [23] Dong W K, Sun Y X, Zhang, Y P, et al. *Inorg. Chim. Acta*, **2009**,**362**:117-124
- [24] Dong W K, Zhang J, Zhang Y, et al. *Inorg. Chem. Acta*, **2016**,**444**:95-102
- [25] Chai L Q, Tang L J, Chen L C, et al. *Polyhedron*, **2017**,**122**: 228-240
- [26] Chai L Q, Zhang K Y, Tang L J, et al. *Polyhedron*, **2017**,**130**: 100-107
- [27] Chen L, Dong W K, Zhang H, et al. *Cryst. Growth Des.*, **2017**,**17**:3636-3648
- [28] LU Rui-E(陆瑞娥), LI Xin-Ran(李新然), ZHAO Ya-Yuan(赵亚元), et al. *Chinese J. Inorg. Chem.*(无机化学学报), **2015**, **31**:1055-1062
- [29] Wang P, Zhao L. *Synth. React. Inorg. Met.-Org. Nano-Met. Chem.*, **2016**,**46**:1095-1101
- [30] Zhao L, Dang X T, Chen Q, et al. *Synth. React. Inorg. Met.-Org. Nano-Met. Chem.*, **2013**,**43**:1241-1246
- [31] Sun Y X, Wang L, Dong X Y, et al. *Synth. React. Inorg. Met.-Org. Nano-Met. Chem.*, **2013**,**43**:599-603
- [32] Dong W K, Ma J C, Zhu L C, et al. *Cryst. Growth Des.*, **2016**,**16**:6903-6915
- [33] DONG Wen-Kui(董文魁), WANG Li(王莉), SUN Yin-Xia(孙银霞), et al. *Chinese J. Inorg. Chem.*(无机化学学报), **2011**,**27**(2):372-376
- [34] Zhang H, Wu H L, Chen C Y, et al. *J. Coord. Chem.*, **2016**, **69**:1577-1586
- [35] Chai, L Q, Liu G, Zhang Y L, et al. *J. Coord. Chem.*, **2013**, **66**:3926-3938
- [36] Duan J G, Liu G L. *Transition Met. Chem.*, **2007**,**32**:702-705
- [37] Dong W K, He X N, Yan H B, et al. *Polyhedron*, **2009**,**28**: 1419-1428

- [38]Dong W K, Feng J H, Wang L, et al. *Transition Met. Chem.*, **2007**,**32**:1101-1105
- [39]Dong W K, Sun Y X, Zhao C Y, et al. *Polyhedron*, **2010**,**29**: 2087-2097
- [40]Li L H, Dong W K, Zhang Y, et al. *Appl. Organomet. Chem.*, **2017**,**31**:e3818
- [41]Li X Y, Chen L, Gao L, et al. *RSC Adv.*, **2017**,**7**:35905-35916
- [42]Song X Q, Wang L, Zheng Q F, et al. *Inorg. Chim. Acta*, **2012**,**391**:171-178
- [43]Hu J H, Sun Y, Qi J, et al. *Spectrochim. Acta A*, **2017**,**175**: 125-133
- [44]Dong X Y, Kang Q P, Jin B X, et al. *Z. Naturforsch.*, **2017**,**72**: 415-420
- [45]Wu H L, Bai Y C, Zhang Y H, et al. *J. Coord. Chem.*, **2014**, **67**:3054-3066
- [46]Wu H L, Pan G L, Bai Y C, et al. *J. Coord. Chem.*, **2013**, **66**:2634-2646
- [47]Jia H R, Li J, Sun Y X, et al. *Z. Krist.: New Cryst. Struct.*, **2018**,**233**(1):45-47
- [48]SAINT-Plus, Ver.6.02, Bruker Analytical X-ray System, Madison, WI, **1999**.
- [49]Sheldrick G M. *SADABS, Program for Empirical Absorption Correction of Area Detector Data*, University of Göttingen, Germany, 1996.
- [50]Sheldrick G M. *SHELXS-97, Program for the Solution and the Refinement of Crystal Structures*, University of Göttingen, Germany, **1997**.
- [51]Sun Y X, Xu L, Zhao T H, et al. *Synth. React. Inorg. Met.-Org. Nano-Met. Chem.*, **2013**,**43**:509-513
- [52]Addison A W, Rao T N, Reedijk J, et al. *J. Chem. Soc. Dalton Trans.*, **1984**,**7**:1349-1356
- [53]Dong W K, Zhang X Y, Sun Y X, et al. *Synth. React. Inorg. Met.-Org. Nano-Met. Chem.*, **2015**,**45**:956-962
- [54]Dong Y J, Li X L, Zhang Y, et al. *Supramol. Chem.*, **2017**, **29**:518-527
- [55]Wang B J, Dong W K, Zhang Y, et al. *Sens. Actuators B: Chem.*, **2017**,**247**:254-264
- [56]Wang L, Hao J, Zhai L X, et al. *Crystals*, **2017**,**7**:277
- [57]Ma J C, Dong X Y, Dong W K, et al. *J. Coord. Chem.*, **2016**, **69**:149-159
- [58]Dong W K, Zhu L C, Dong Y J, et al. *Polyhedron*, **2016**,**117**: 148-154
- [59]Xu L, Zhu L C, Ma J C, et al. *Z. Anorg. Allg. Chem.*, **2015**, **641**:2520-2524
- [60]Dong W K, Wang Z K, Li G, et al. *Z. Anorg. Allg. Chem.*, **2013**,**639**:2263-2268
- [61]Chai L Q, Huang J J, Zhang J Y, et al. *J. Coord. Chem.*, **2015**,**68**:1224-1237
- [62]Wang L, Ma J C, Dong W K, et al. *Z. Anorg. Allg. Chem.*, **2016**,**642**:834-839
- [63]Wang P, Zhao L. *Asian J. Chem.*, **2015**,**4**:1424-1426
- [64]Dong Y J, Ma J C, Zhu L C, et al. *J. Coord. Chem.*, **2017**,**70**: 103-115
- [65]Chai L Q, Wang G, Sun Y X, et al. *J. Coord. Chem.*, **2012**, **65**:1621-1631
- [66]Wu H L, Bai Y, Yuan J K, et al. *J. Coord. Chem.*, **2012**,**65**: 2839-2851
- [67]Wu H L, Pan G L, Bai Y C, et al. *J. Photochem. Photobiol. B*, **2014**,**135**:33-43
- [68]Song X Q, Peng Y J, Chen G Q, et al. *Inorg. Chim. Acta*, **2015**,**427**:13-21
- [69]Hu J H, Li J B, Qi J, et al. *New J. Chem.*, **2015**,**39**:843-848
- [70]Liu P P, Wang C Y, Zhang M, et al. *Polyhedron*, **2017**,**129**: 133-140
- [71]Chai L Q, Zhang H S, Huang J J, et al. *Spectrochim. Acta A*, **2015**,**137**:661-669
- [72]Dong W K, Zhang F, Li N. *Z. Anorg. Allg. Chem.*, **2016**,**642**: 532-538
- [73]Wang P, Zhao L. *Spectrochim. Acta Part A*, **2015**,**135**:342-350
- [74]Gao L, Wang F, Zhao Q, et al. *Polyhedron*, **2018**,**139**:7-16
- [75]Dong W K, Ma J C, Dong Y J, et al. *J. Coord. Chem.*, **2016**, **69**:3231-3241
- [76]Wu H L, Huang X C, Yuan J K, et al. *Z. Naturforsch.*, **2011**, **66b**:1049-1055
- [77]Wu H L, Li K, Sun T, et al. *Transition Met. Chem.*, **2011**,**36**: 21-28
- [78]Wu H L, Wang K. T, Kou F, et al. *J. Coord. Chem.*, **2010**, **64**:2676-2687
- [79]Zhang Y G, Shi Z H, Yang L Z, et al. *Inorg. Chem. Commun.*, **2014**,**39**:86-89
- [80]Wang F, Gao L, Zhao Q, et al. *Spectrochim. Acta Part A*, **2018**,**190**:111-115
- [81]Dong W K, Akogun S F, Zhang Y, et al. *Sens. Actuators B: Chem.*, **2017**,**238**:723-734
- [82]Song X Q, Cheng G Q, Liu Y A. *Inorg. Chim. Acta*, **2016**, **450**:386-394
- [83]Zheng S S, Dong W K, Zhang Y, et al. *New J. Chem.*, **2017**, **41**:4966-4973
- [84]Song X Q, Liu P P, Liu Y A, et al. *Dalton Trans.*, **2016**,**45**: 8154-8163
- [85]Wang L, Zhao Q, Li X Y, et al. *Z. Naturforsch. B*, **2017**,**72** (12):947-953